Harnessing the catalytic potential of a ferulic acid esterase for MHET hydrolysis

P. Karampa[1], K. Makryniotis[2], E. Nikolaivits[2], V. Daskalakis[3], E. Topakas[2], M. Dimarogona[1]*

[1] Laboratory of Structural Biology and Biotechnology, Department of Chemical Engineering, University of Patras, Patras, Greece,
[2] Industrial Biotechnology & Biocatalysis Group, Biotechnology Laboratory, School of Chemical Engineering, National Technical University of Athens, Athens, Greece,
[3] Laboratory of Biomolecular Dynamics and Engineering, Department of Chemical Engineering, University of Patras, Patras, Greece
(* mdimarog@chemeng.upatras.gr)

Introduction

Polyethylene terephthalate (PET) is one of the most common polymers used in packaging, construction, and agricultural industries [1,2]. Its semi-aromatic and semi-crystalline synthesis gives it high mechanical strength and barrier properties suitable for packaging. Many enzymes that decompose PET have been discovered since 2000, such as lipases and carboxyl ester hydrolases [3]. Both PET and MHET hydrolases attack the polymer ester bonds (Fig. 1) [4].

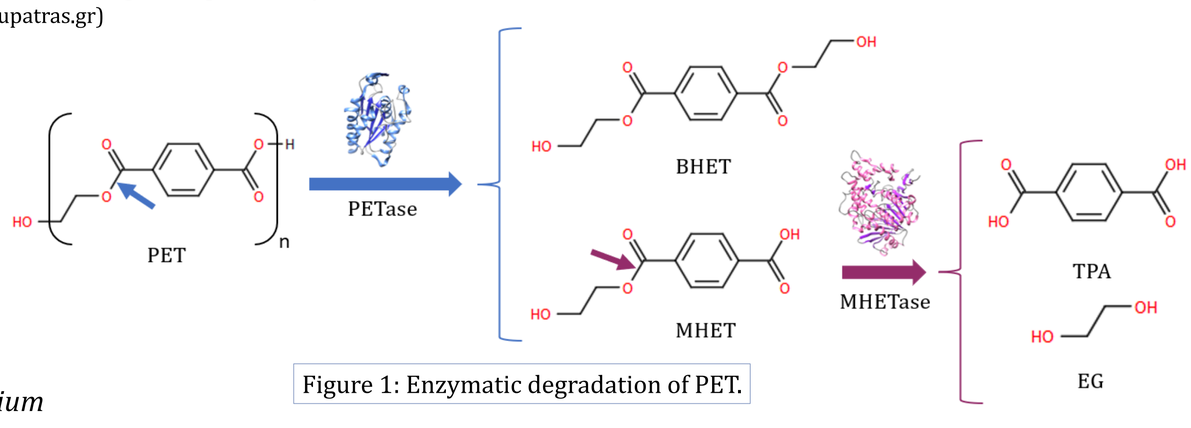

Figure 1: Enzymatic degradation of PET.

Objectives

This study focuses on investigation of structure-function relations of a ferulic acid esterase from *Fusarium oxysporum* (*Fo*FaeC) with degradation capacity against MHET [5]. Using structure-guided mutagenesis to mimick MHETase active site, an *Fo*FaeC variant, G122S, was created. The aim was to identify the structural determinants of MHETase activity by combining:

1. The determination of crystal structure of *Fo*FaeC variant, and
2. Molecular Dynamics (MD) and Docking Simulations of both wild-type *Fo*FaeC and its variant.

X-ray Crystallography

Methodology: *Fo*FaeC variant was expressed in *Pichia pastoris* and purified using immobilized metal affinity chromatography. A mixture of 16mg/ml G122S and 5mM MHET, after 30min incubation on ice, was used for crystallization using sitting drop, vapor – diffusion method in the presence of already established crystallization condition [6,7].

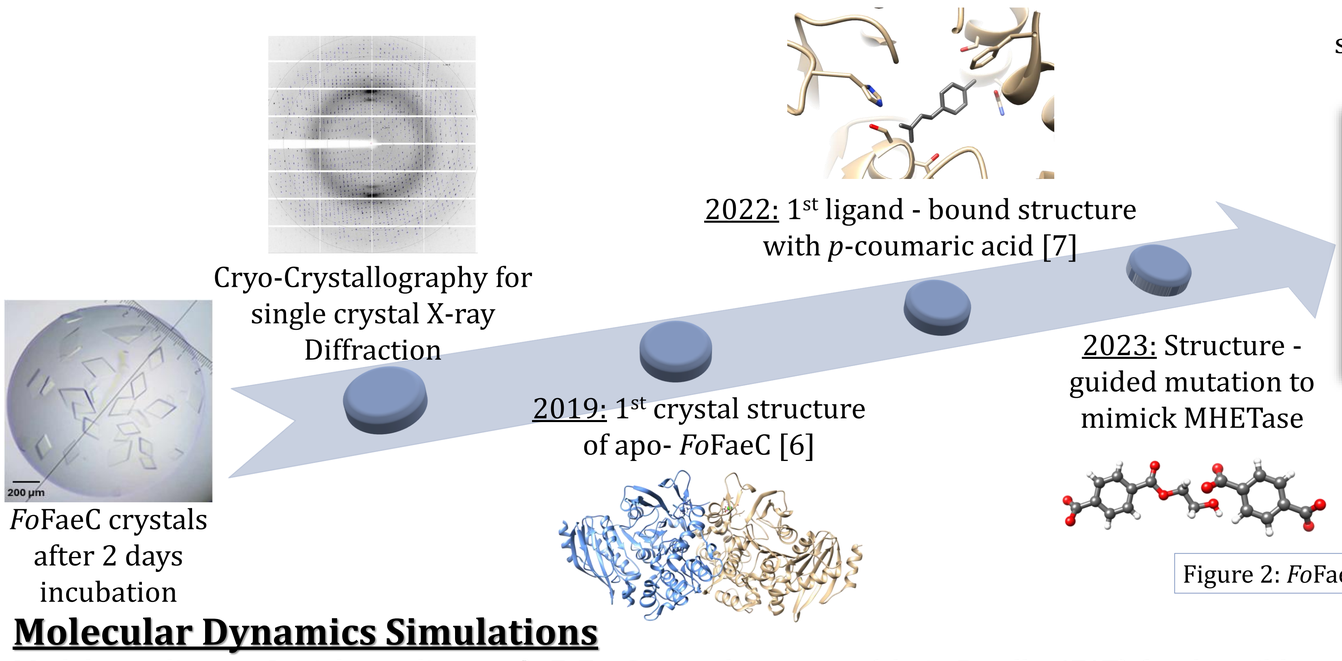

Figure 2: *Fo*FaeC structural studies.

Table 1: Diffraction data and refinement statistics for *Fo*FaeC_G122S structure. Values in parenthesis is for the outermost shell.

Data Collection		Multiplicity	3.4 (3.4)
Beamline	P13	No. of observations	491 252 (24 257)
Wavelength (Å)	0.9763	Unique reflections	143 024 (7131)
Space group	$P2_1$	R_{merge} (%)	0.074 (0.645)
Unit Cell Parameters		R_{pim} (%)	0.046 (0.409)
(a, b, c) (Å)	(68.0, 89.9, 115.1)	**Refinement Statistics**	
Resolution (Å)	89.93-1.71 (1.74-1.71)	R_{work} (%)	0.179
Completeness (%)	98.6 (99.2)	R_{free} (%)	0.208
Mean (I/SD(I))	7.5 (1.5)	RMSD, bond length (Å)	0.0103
$CC_{1/2}$	0.995 (0.812)	RMSD, bond angles (o)	1.912

Molecular Dynamics Simulations

Model coordinates: Initial coordinates → *Fo*FaeC crystal structure (chain B, pdb: 6FAT) for the wild-type (WT) and from the crystallographic experiments for the mutant G122S (MT). The model structures were embedded in a 12x12x12 nm^3 simulation box – cell and hydrated with TIP3P water molecules [9]. The models contained one structural Ca^{2+} and 5 Cl^- anions to neutralize the system (~173k atoms in total). The Charmm36 Force Field was employed for the description of the polypeptide chains and ions [10]. MD simulations were performed in GROMACS v 2022.5 MD engine.

Model equilibration: Based on published protocols, all models were relaxed and equilibrated with gradual removal of constraints on the protein backbone-heavy atoms [11]. This totals in a production **sampling time** of 2 systems (WT, MT) x 4 (independent trajectories)/ system x 0.5μs = **4μs**.

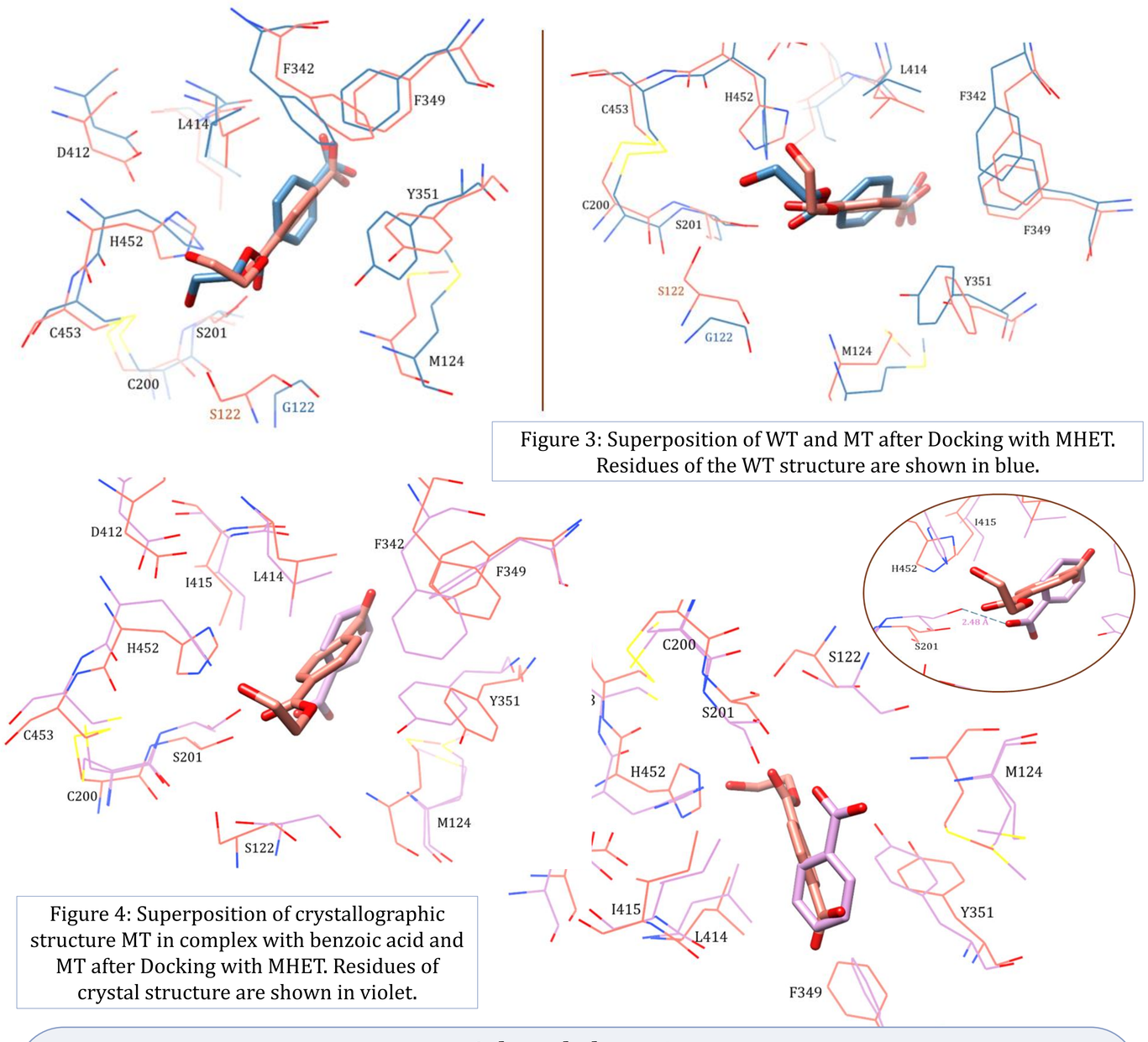

Figure 3: Superposition of WT and MT after Docking with MHET. Residues of the WT structure are shown in blue.

Figure 4: Superposition of crystallographic structure MT in complex with benzoic acid and MT after Docking with MHET. Residues of crystal structure are shown in violet.

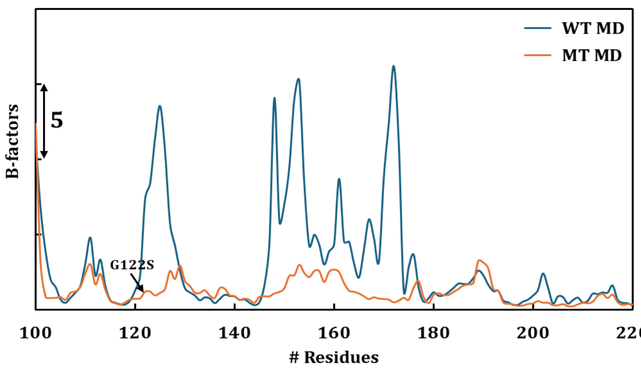

Diagram 1: Comparison between B-factors of wild-type *Fo*FaeC and G122S focusing on the region of mutation after 0.5μs MD simulation.

Table 2: Docking analysis of WT and MT.

WT structures with MHET	
Average Binding Energy (kcal/mol)	5.068
Standard Deviation	0.321
MT structures with MHET	
Average Binding Energy (kcal/mol)	5.153
Standard Deviation	0.208

Docking with MHET

Docking analysis was performed using the YASARA 21.6.17 software. Key conformations for *Fo*FaeC enzyme (WT and MT) were obtained from the MD analysis and the ligand was downloaded from the PDB (PBD code: 6QGA). The structure superimposed using MUSTANG and the resulting structure was used to perform local docking in YASARA. The absolute values of binding energy are shown in Table 2 (higher values indicates stronger binding).

Conclusions – Future work

- First crystal structure of *Fo*FaeC variant (G122S) in complex with benzoic acid.
- Reduced mobility in the region around residues 100 – 200 due to the mutation G122S contributes to increased *Fo*FaeC activity against MHET.
- Docking confirms the enhanced binding of MHET in the active site of G122S variant.
- The decreased standard deviation of binding energies of MHET at the catalytic center of MT structures indicates an energetically more stable conformation.
- Currently, MD simulation of docking structures is in progress.

Acknowledgments

We would like to thank the staff at beamlines P13 (PETRA III, EMBL Hamburg) and 14.1 at (BESSY II, HZB Berlin) for help during data collection. We would also like to thank iNEXT Discovery for providing financial support for synchrotron data collection. The simulations were performed on the Luxemburg national supercomputer MeluXina. V.D. gratefully acknowledges the LuxProvide teams for their expert support. The research work was supported by the Basic Research Financing (Horizontal support for all Sciences), Hellenic Foundation for Research and Innovation (H.F.R.I.) under the "2nd Call for H.F.R.I. Research Projects to support Faculty members and Researchers" (PlastOmics, project number: 03061) and National Recovery and Resilience Plan (Greece 2.0) Action, under the "Sub-action II Funding Projects in Leading-Edge Sectors" (EnZyReMix, project number: 15024).

References

1. Urbanek, A. K., Kosiorowska, K. E., & Mironczuk, A. M. (2021). Current Knowledge on Polyethylene Terephthalate Degradation by Genetically Modified Microorganisms. Frontiers in Bioengineering and Biotechnology. 9:771133.
2. Rüthi, J., Cerri, M., Brunner, I., Stierli, B., Sander, M., & Frey, B. (2023). Discovery of plastic-degrading microbial strains isolated from the alpine and Arctic terrestrial pastisphere. Frontiers in Microbiology. 14:1178474. doi: 10.3389/fmicb.2023.1178474.
3. Tournier, V., Duquesne, S., Guillamot, Fr., Cramail, H., Taton, D., Marty, A., & Andre, I. (2023). Enzymes' Power for Plastics Degradation. ACS Publications. Chemical Reviews, 123 (9): 5612-5701.
4. Yoshida, Sh., Hiraga, K., Taniguchi, I., & Oda, K. (2021). Chapter Nine - Ideonella sakaiensis, PETase and MHETase: From identification of microbial PET degradation to enzyme characterization. Methods in Enzymology. Academic Press. Vol. 648: 187-205.
5. Taxeidis, G., Djapovic, M., Nikolaivits, E., Maslak, V., Nikodinovic-Runic, J., & Topakas, E. (2024). New labeled PET analogues enable the functional screening and characterization of PET-degrading enzymes. ACS Sustainable Chemistry & Engineering. 12 (15): 5943-5952.
6. Dimarogona, M., Topakas, E., Christakopoulos, P., & Chrysina, E. D. (2020). The crystal structure of a Fusarium oxysporum feruloyl esterase that belongs to the tannase family. FEBS Letters, 594: 1738-1749.
7. Ferousi, Ch., Kosinas, Ch., Nikolaivits, E., Topakas, E., & Dimarogona, M. (2023). Crystal structure of the Fusarium oxysporum tannase-like feruloyl esterase FaeC in complex with p-coumaric acid provides insight into ligand binding. FEBS Letters, 597: 1415-1427.
8. Sagong, H.-Y., Seo, H., Kim, T., Son, H., Joo, S., Lee, S., Kim, S., Woo, J.-S., Hwang, S., & Kim, K.-J. (2020). Decomposition of PET film by MHETase using Exo-PETase function. ACS Catalysis, 10: 4805-4812.
9. Mark P, Nilsson L (2001) Structure and dynamics of the TIP3P, SPC, and SPC/E water models at 298 K. Journal of Physical Chemistry A 105:9954–9960. https://doi.org/10.1021/jp003020w
10. Lindahl E, Bjelkmar P, Larsson P, et al (2010) Implementation of the charmm force field in GROMACS: Analysis of protein stability effects from correction maps, virtual interaction sites, and water models. J Chem Theory Comput 6:459–466. https://doi.org/10.1021/ct900549r
11. Petratos K, Gessmann R, Daskalakis V, et al (2020) Structure and Dynamics of a Thermostable Alcohol Dehydrogenase from the Antarctic Psychrophile Moraxella sp. TAE123. ACS Omega. https://doi.org/10.1021/acsomega.0c01210